SCIENCE CHINA
Physics, Mechanics & Astronomy

• Article •

January 2012 Vol.55 No.1: 66–77
doi: 10.1007/s11433-011-4570-z

A collocation interval analysis method for interval structural parameters and stochastic excitation

QI WuChao* & QIU ZhiPing

Institute of Solid Mechanics, Beijing University of Aeronautics and Astronautics, Beijing 100191, China

Received April 8, 2011; accepted October 31, 2011; published online December 15, 2011

Uncertainty propagation, one of the structural engineering problems, is receiving increasing attention owing to the fact that most significant loads are random in nature and structural parameters are typically subject to variation. In the study, the collocation interval analysis method based on the first class Chebyshev polynomial approximation is presented to investigate the least favorable responses and the most favorable responses of interval-parameter structures under random excitations. Compared with the interval analysis method based on the first order Taylor expansion, in which only information including the function value and derivative at midpoint is used, the collocation interval analysis method is a non-gradient algorithm using several collocation points which improve the precision of results owing to better approximation of a response function. The pseudo excitation method is introduced to the solving procedure to transform the random problem into a deterministic problem. To validate the procedure, we present numerical results concerning a building under seismic ground motion and aerofoil under continuous atmosphere turbulence to show the effectiveness of the collocation interval analysis method.

uncertainty propagation, interval analysis, Taylor series expansion, Chebyshev polynomial, Pseudo excitation method

PACS number(s): 02.30.Mv, 02.50Ey, 02.60Gf, 02.70.Jn

Citation: Qi W C, Qiu Z P. A collocation interval analysis method for interval structural parameters and stochastic excitation. Sci China-Phys Mech Astron, 2012, 55: 66–77, doi: 10.1007/s11433-011-4570-z

The treatment of structural parameters and external excitations as uncertain variables has been the research subject of engineers and scientists for many years [1]. The concept of uncertainty plays an important role in the investigation of various science and engineering problems. The uncertainties in structural systems affect design and operating performance to a large extent. In structural static and dynamical analysis, the structural parameters are usually subject to variation due to fluctuations in material properties, uncertainty in boundary conditions, and variations caused by manufacturing and assembly techniques. In the current literature regarding structural response problems with random uncertainties, there are three main methods [2]: the Monte Carlo simulation method [3–6], the stochastic finite element method [7–10], and the orthogonal series expansion method [11,12]. The Monte Carlo simulation method is very efficient in the aspect of structural random analysis, but it is quite time-consuming. The stochastic finite element method is very powerful in solving the random eigen problem, static analysis problem, and structural stability problem, but the method is haunted by the notorious secular term in structural random dynamical response analysis. According to the orthogonal series expansion method, the structural response may be expanded into an orthogonal series, and the corresponding numerical characteristics are given as the analytical solution form. Unfortunately, despite the success of the above probabilistic analysis approaches, the probabilistic approach requires a wealth of data, often unavailable, in order to define the probability distribution density. When crucial information for describing variability is missing, it is not good practice to model the uncertainties as a probabilis-

*Corresponding author (email: qiwuchao@ase.buaa.edu.cn)

tic quantity [13]. In the frequently encountered case where sufficient knowledge about the external excitations and structural parameters is absent for substantiation of the stochastic analysis, an alternative method models uncertainties on the basis of non-probabilistic conceptual frameworks. These approaches are based on set-theoretical formulations by adopting convex models or interval analysis methods [14–23] in which only the bounds on the magnitude of uncertain external excitations and parameters are required, not necessarily knowledge concerning the probabilistic distribution densities. The interval analysis method models the uncertainty quantities as interval variables with lower and upper bounds. In the case of the uncertainty being slight, the so-called interval perturbation method [15], and interval analysis method based on the first order Taylor expansion [19,20] can be adopted in both static and dynamic analysis. These methods are advantageous mainly in their flexibility and simplicity of the mathematical formulation. However, the effectiveness of these methods is limited due to the assumption of small intervals. Since the method is based on the first order sensitivity at the nominal point, the obtained range of response function is related to the accuracy of the first order sensitivity. When an uncertain variable is not located in a small interval, or the response function varies in the width range, the method can't be executed. In the study, a new interval analysis method named the collocation interval analysis method (which doesn't depend on sensitivity) is presented. This method can be applied when the uncertain variable lies in the width range and will not suffer the assumption of small interval.

On the other hand, over the last few decades, researchers have recognized that most significant loads, such as seismic ground motion, gusty winds, sea waves, jet noise, etc., involved in structural engineering problems are random in nature. These excitations can be modeled as stochastic processes. A stationary stochastic process can be calculated relatively easily and has widespread availability in engineering. The second-order stochastic process, where the mean-value function and variance function are finite, can be used to describe mostly real processes. An accurate and highly efficient algorithm known as the Pseudo-excitation method [24–27], has been developed for the random vibration computation of complex engineering structures. The difficulty in computational efforts for the stationary and non-stationary random response can be satisfactorily overcome. The cross-correlation terms between all participant modes and all random excitations have been included. Therefore, the Pseudo-excitation method is a Complete Quadratic Combination (CQC) method.

In the literature, interval analysis methods have been developed to evaluate the static response and dynamic analysis of structures with interval parameters subject to deterministic excitations. However, to the authors' best knowledge, interval methods have never been applied to evaluate the response of structural systems with interval parameters under stochastic process input. In the design of engineering structures, incorporation of uncertainties of structural parameters and randomness of loads should therefore result in more efficient designs.

The aim of the paper is to evaluate the range of the stochastic response statistics of linear structural systems with interval parameters subjected to stochastic excitations. The mean value function can be adjusted to zero through centralizing the stochastic process. Therefore, obtaining the bounds of the auto-power spectrum density (PSD) function and variance function of the response function is the main objective in the study. Numerical results concerning a building under seismic ground motion and aerofoil under continuous atmosphere turbulence are presented to show the effectiveness of the proposed method.

1 Problem statement

Consider the equation of motion of a general dynamical system with n degrees of freedom in the following form:

$$\boldsymbol{M}\ddot{\boldsymbol{x}}(t)+\boldsymbol{C}\dot{\boldsymbol{x}}(t)+\boldsymbol{K}\boldsymbol{x}(t)=\boldsymbol{F}(t), \tag{1}$$

where $\boldsymbol{x}(t)=(x_i(t))$, $\dot{\boldsymbol{x}}(t)=(\dot{x}_i(t))$ and $\ddot{\boldsymbol{x}}(t)=(\ddot{x}_i(t))$ are the displacement, velocity and acceleration vectors, and the mass matrix $\boldsymbol{M}=(m_{ij})$, the damping matrix $\boldsymbol{C}=(c_{ij})$ and the stiffness matrix $\boldsymbol{K}=(k_{ij})$ depend on the structural parameter vector $\boldsymbol{h}=(h_i)$ and may be expressed as functions of the structural parameter vector $\boldsymbol{h}$, i.e.,

$$\begin{aligned}\boldsymbol{M}&=\boldsymbol{M}(\boldsymbol{h})=(m_{ij}(\boldsymbol{h})),\\ \boldsymbol{C}&=\boldsymbol{C}(\boldsymbol{h})=(c_{ij}(\boldsymbol{h})),\\ \boldsymbol{K}&=\boldsymbol{K}(\boldsymbol{h})=(k_{ij}(\boldsymbol{h}))\end{aligned} \tag{2}$$

in which $\boldsymbol{h}=(h_i)$ is m-dimensional vector. $\boldsymbol{F}(t)=(f_i(t))$ is a stochastic load vector with no specific expression but known PSD function $S_{FF}(\omega)=(S_{f_if_j}(\omega))$. Thus, eq. (1) can be rewritten as:

$$\boldsymbol{M}(\boldsymbol{h})\ddot{\boldsymbol{x}}(\boldsymbol{h},t)+\boldsymbol{C}(\boldsymbol{h})\dot{\boldsymbol{x}}(\boldsymbol{h},t)+\boldsymbol{K}(\boldsymbol{h})\boldsymbol{x}(\boldsymbol{h},t)=\boldsymbol{F}(t). \tag{3}$$

Considering a realistic situation in which available information on the structural parameter vector $\boldsymbol{h}=(h_i)$ is not enough to justify an assumption on its probabilistic characteristics, we follow the thought of interval mathematics and assume that the structural parameter vector $h=(h_i)$ belongs to a bounded interval vector:

$$\boldsymbol{h}\in\boldsymbol{h}^I=[\underline{\boldsymbol{h}},\overline{\boldsymbol{h}}]=(h_i^I),\quad h_i\in h_i^I=[\underline{h}_i,\overline{h}_i],\quad i=1,2,\cdots,m, \tag{4}$$

where $\overline{\boldsymbol{h}}=(\overline{h}_i)$ and $\underline{\boldsymbol{h}}=(\underline{h}_i)$ are the upper and lower bounds of structural parameters $\boldsymbol{h}=(h_i)$, respectively. From interval mathematics, we know that eq. (3) describes a 'box' with m order of dimension.

Our aim is to find statistics of all the possible dynamical responses $\boldsymbol{x}(t)$ satisfying the dynamical equation (3), where $\boldsymbol{h}$ is assumed to be all possible values inside the interval parameter vector $\boldsymbol{h}^I$. This infinite number of statistics of dynamical responses constitutes bounded sets Γ which has a very complicated region in general. In the sense of interval mathematics, the aim is seeking the upper and lower bounds of the auto PSD function and the variance function, i.e.

$$S^I_{x_i x_i}(\omega)=\left[\underline{S}_{x_i x_i}(\omega),\overline{S}_{x_i x_i}(\omega)\right]=\left(S^I_i(\omega)\right),\quad i=1,2,\cdots,n, \tag{5}$$

$$\sigma^I_{x_i}(t)=\left[\underline{\sigma}_{x_i}(t),\overline{\sigma}_{x_i}(t)\right]=\left(\sigma^I_i(t)\right),\quad i=1,2,\cdots,n, \tag{6}$$

where ω is an angular frequency variable.

2 Pseudo excitation method

For deterministic structural systems with stochastic process inputs, the PSD matrix of response function of multi-input and multi-output system can be expressed as:

$$\boldsymbol{S}_{xx}(\omega)=\boldsymbol{H}^*(\omega)\boldsymbol{S}_{FF}(\omega)\boldsymbol{H}^{\mathrm{T}}(\omega), \tag{7}$$

where $H(\omega)$ is the frequency transfer function matrix, the superscript '*' and 'T' are adjoint operator and transposed operator, respectively. Though eq. (7) is extensively used in engineering, it is necessary to choose many discrete frequency points to execute matrix multiplication twice, which results in rather low efficiency for large structural systems. For this reason, the modal superposition method and pseudo excitation method are introduced to increase the computational efficiency. Thus the pseudo response vector can be constructed as follows:

$$\tilde{\boldsymbol{x}}(\omega,t)=\sum_{j=1}^{q}\gamma_j H_j(\omega)\boldsymbol{\phi}_j\sqrt{S_{g_j}(\omega)}\mathrm{e}^{\mathrm{i}\omega t}, \tag{8}$$

where the superscript '~' represents pseudo quantity, q is the number of truncated modal orders, γ_j, $\boldsymbol{\phi}_j$ are the jth mode factor and modal vector, and $g_j(t)$ may be the linear combination of the components of $\boldsymbol{F}(t)$. Based on eq. (8), we can get

$$\begin{aligned}\boldsymbol{S}_{xx}(\omega)=\tilde{\boldsymbol{x}}^*\tilde{\boldsymbol{x}}^{\mathrm{T}}&=\left(\sum_{j=1}^{q}\gamma_j H_j(\omega)\boldsymbol{\phi}_j\sqrt{S_{g_j}(\omega)}\right)^*\\&\times\left(\sum_{k=1}^{q}\gamma_k H_k(\omega)\boldsymbol{\phi}_k\sqrt{S_{g_k}(\omega)}\right)^{\mathrm{T}}.\end{aligned} \tag{9}$$

It can be proved that eq. (9) is an equivalent to eq. (7) when $q=n$. Pseudo excitation method avoids the computational effort on double summation and transforms a random vibration problem into a determinate problem. Only one vector multiplication is needed to obtain the power spectrum matrix of the response function. It can greatly improve the computational efficiency, and can be implemented for the calculation of large complex structures. In the study, this method is used to solve stochastic statistics in the sequence sections.

3 Interval analysis method based on taylor expansion (TIAM) under stationary Stochastic excitation

In this section, we first define the nominal value vector of the interval structural parameter vector as:

$$\boldsymbol{h}^c=(\boldsymbol{h}^c_i)=m(h^I)=\frac{(\overline{\boldsymbol{h}}+\underline{\boldsymbol{h}})}{2},\quad i=1,2,\cdots,m. \tag{10}$$

and the deviation amplitude vector or the uncertain radius vector of the interval structural parameter vector as:

$$\Delta\boldsymbol{h}=(\Delta h_i)=\mathrm{rad}(\boldsymbol{h}^I)=\frac{(\overline{\boldsymbol{h}}-\underline{\boldsymbol{h}})}{2},\quad i=1,2,\cdots,m. \tag{11}$$

Thus, based on interval mathematics, the interval structural parameter vector is decomposed into the sum of the nominal value vector and the deviation vector, i.e.

$$\begin{aligned}\boldsymbol{h}^I&=\left[\underline{\boldsymbol{h}},\overline{\boldsymbol{h}}\right]=\left[\boldsymbol{h}^c-\Delta\boldsymbol{h},\boldsymbol{h}^c+\Delta\boldsymbol{h}\right]\\&=\boldsymbol{h}^c+\Delta\boldsymbol{h}^I=\boldsymbol{h}^c+\Delta\boldsymbol{h}\left[-1,1\right]=\boldsymbol{h}^c+\Delta\boldsymbol{h}e_\Delta,\end{aligned} \tag{12}$$

where $e_\Delta=[-1,1]$.

In terms of expression (12), the interval structural parameter vector may be written in the following form:

$$\boldsymbol{h}=\boldsymbol{h}^c+\delta\boldsymbol{h},\quad \left|\delta\boldsymbol{h}\right|\leqslant\Delta\boldsymbol{h}. \tag{13}$$

When structural system contains uncertain variances which are characterized by interval vector $\boldsymbol{h}$, pseudo dynamic response eq. (8) and the corresponding PSD function can be rewritten as:

$$\tilde{\boldsymbol{x}}(\boldsymbol{h},\omega,t)=\sum_{j=1}^{q}\gamma_j(\boldsymbol{h})H_j(\boldsymbol{h},\omega)\boldsymbol{\phi}_j(\boldsymbol{h})\sqrt{S_{g_i}(\omega)}\mathrm{e}^{\mathrm{i}\omega t} \tag{14}$$

and

$$\begin{aligned}\boldsymbol{S}_{xx}(\boldsymbol{h},\omega)&=\tilde{\boldsymbol{x}}^*\tilde{\boldsymbol{x}}^{\mathrm{T}}\\&=\left(\sum_{j=1}^{q}\gamma_j(\boldsymbol{h})H_j(\boldsymbol{h},\omega)\boldsymbol{\phi}_j(\boldsymbol{h})\sqrt{S_{g_i}(\omega)}\right)^*\\&\times\left(\sum_{k=1}^{q}\gamma_k(\boldsymbol{h})H_k(\boldsymbol{h},\omega)\boldsymbol{\phi}_k(\boldsymbol{h})\sqrt{S_{g_k}(\omega)}\right)^{\mathrm{T}}.\end{aligned} \tag{15}$$

Fixing frequency ω on the concerned frequency point $\omega=\omega_c$, $\boldsymbol{S}_{xx}(\boldsymbol{h},\omega)$ in eq. (15) is only the function of interval vector h, as:

$$\boldsymbol{S}_{xx}(\boldsymbol{h},\omega_c)=\tilde{\boldsymbol{x}}^*\tilde{\boldsymbol{x}}^{\mathrm{T}}=\left(\sum_{j=1}^{q}\gamma_j(\boldsymbol{h})H_j(\boldsymbol{h},\omega_c)\boldsymbol{\phi}_j(\boldsymbol{h})\sqrt{S_{g_i}(\omega_c)}\right)^*$$

$$\times\left(\sum_{k=1}^{q}\gamma_k(\boldsymbol{h})H_k(\boldsymbol{h},\omega_c)\phi_k(\boldsymbol{h})\sqrt{S_{g_k}(\omega_c)}\right)^{\mathrm{T}}. \quad (16)$$

Using Taylor series expansion to the first order at the nominal value point, the component form $S_{x_ix_i}(\boldsymbol{h},\omega_c)$ can be expressed approximately as follows:

$$S_{x_ix_i}(\boldsymbol{h},\omega_c)=S_{x_ix_i}(\boldsymbol{h}^c,\omega_c)+\sum_{k=1}^{m}\frac{\partial S_{x_ix_i}(\boldsymbol{h}^c,\omega_c)}{\partial h_k}\delta h_k, \quad (17)$$

in which

$$\delta h_k\in\Delta h_k^I=\left[-\Delta h_k,\Delta h_k\right],\ \ k=1,2,\cdots,m. \quad (18)$$

By using the interval extension in interval mathematics, the interval extension of the component of PSD function matrix can be obtained from eq. (17), as:

$$S_{x_ix_i}^I(\boldsymbol{h},\omega_c)=S_{x_ix_i}(\boldsymbol{h}^c,\omega_c)+\sum_{k=1}^{m}\left|\frac{\partial S_{x_ix_i}(\boldsymbol{h}^c,\omega_c)}{\partial h_k}\right|\Delta h_k^I. \quad (19)$$

After the interval operations, from the above equation, we have

$$\overline{S}_{x_ix_i}(\boldsymbol{h},\omega_c)=S_{x_ix_i}(\boldsymbol{h}^c,\omega_c)+\sum_{k=1}^{m}\left|\frac{\partial S_{x_ix_i}(\boldsymbol{h}^c,\omega_c)}{\partial h_k}\right|\Delta h_k \quad (20)$$

and

$$\underline{S}_{x_ix_i}(\boldsymbol{h},\omega_c)=S_{x_ix_i}(\boldsymbol{h}^c,\omega_c)-\sum_{k=1}^{m}\left|\frac{\partial S_{x_ix_i}(\boldsymbol{h}^c,\omega_c)}{\partial h_k}\right|\Delta h_k. \quad (21)$$

By eqs. (20) and (21) we can determine the interval region of the PSD matrix at the concerned frequency point $\omega=\omega_c$.

It should be noted that it is necessary to obtain the sensitivities of the component of PSD function matrix with respect to different interval variables in eqs. (17), (19)–(21). An alternative approach in engineering simply replaces differential calculus into differences calculus, as:

$$\frac{\partial S_{x_ix_i}(\boldsymbol{h}^c,\omega_c)}{\partial h_k}\approx\frac{S_{x_ix_i}(\boldsymbol{h}^c+\delta^k\boldsymbol{h}^c,\omega_c)-S_{x_ix_i}(\boldsymbol{h}^c,\omega_c)}{\delta^k\boldsymbol{h}^c} \quad (22)$$

in which $\delta^k\boldsymbol{h}^c$ represents only perturbing the k-th variable in vector $\boldsymbol{h}^c$. And now, the components $S_{x_ix_j}(\boldsymbol{h}^c,\omega_c)$ and $S_{x_ix_j}(\boldsymbol{h}^c+\delta^k\boldsymbol{h}^c,\omega_c)$ can all be determined by solving the deterministic structural parameters system. Substituting eq. (22) into eqs. (20) and (21), we can obtain the interval bounds of the PSD matrix at the concerned frequency point $\omega=\omega_c$, as:

$$\overline{S}_{x_ix_i}(\boldsymbol{h},\omega_c)=S_{x_ix_i}(\boldsymbol{h}^c,\omega_c)+\sum_{k=1}^{m}\left|\frac{S_{x_ix_i}(\boldsymbol{h}^c+\delta^k\boldsymbol{h}^c,\omega_c)-S_{x_ix_i}(\boldsymbol{h}^c,\omega_c)}{\delta^k\boldsymbol{h}^c}\right|\Delta h_k \quad (23)$$

and

$$\underline{S}_{x_ix_i}(\boldsymbol{h},\omega_c)=S_{x_ix_i}(\boldsymbol{h}^c,\omega_c)-\sum_{k=1}^{m}\left|\frac{S_{x_ix_i}(\boldsymbol{h}^c+\delta^k\boldsymbol{h}^c,\omega_c)-S_{x_ix_i}(\boldsymbol{h}^c,\omega_c)}{\delta^k\boldsymbol{h}^c}\right|\Delta h_k. \quad (24)$$

The significant merit of interval analysis based on the Taylor expansion is that it is simple and efficient. Only statistics values and sensitivities of statistics values with respect to each interval variable at nominal value are necessary. When the number of the interval variables is m, the first order method can estimate statistics' bounds through solving deterministic problems by m+1 times.

Despite its computational efficiency, its shortcomings are obvious. First, the bounds estimated by the first order method are usually different from the bounds of the true region. For example, if the objective function is monotonic in the range of uncertain variables, as Figure 1, it is obvious that one of the bounds goes over the true bound, and the other one is lower than the true bound. Owing to estimated bounds, which use the relatively inaccurate first order method, the bounds obtained from eqs. (23) and (24) are a 'rough' assessment. In general, one can't guarantee that the estimated interval contains the true interval. In other words, the structures designed according to the first order method are not necessarily accurate.

4 Collocation interval analysis method (CIAM) under stationary Stochastic excitation

The approximate formula of Taylor expansion involves

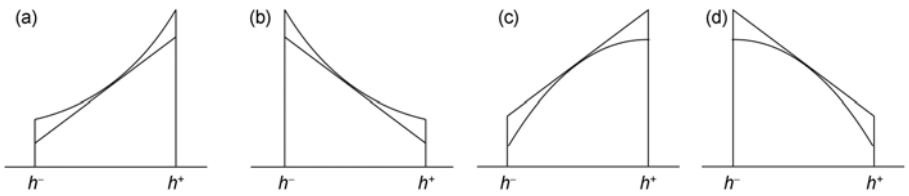

Figure 1 The approximation formula of the first order method with respect to the objective function. (a) Monotonic increasing lower convex function; (b) monotonic decreasing lower convex function; (c) monotonic increasing upper convec function; (d) monotonic decreasing upper convec function.

solving a response function value and derivatives at the center of a super rectangular bounding with interval variables, and spans an approximate surface of a real response function according to the central point's information. In other words, the interval analysis methods based on Taylor expansion only use the central point's information to evaluate the maximum and minimum values of the real response function when, in fact, we can use the other points' information to do this work.

Except for Taylor expansion, one can use another approximate method to describe the real response function with much higher accuracy. Researchers in the field of function approximation have discussed using a series of simple functions $\{p(x)\}$ to approximate a continuous function located on a closed interval. Function's Chebyshev orthogonal polynomial expansion is usually used for function's approximate calculation in the whole interval; it is called 'the most economic expansion'. In the study, the first class Chebyshev polynomial is used to approximate the response function. The coefficients of expansion equation can be obtained from the Gauss-Chebyshev quadrature formula through collocating Gauss quadrature points in the interval of uncertain variables. For each interval variable, one can obtain the extreme points' distribution of the approximate function. Then we can get a maximum point and a minimum point at which the objective function reaches the maximum value and minimum value.

4.1 Collocation interval analysis method

According to eq. (12), we can rewrite interval vector $\boldsymbol{h}$ as:

$$\boldsymbol{h} = \boldsymbol{h}^c + \Delta\boldsymbol{h} * \boldsymbol{e}, \tag{25}$$

where $\boldsymbol{e}$ is one such vector whose absolute value of the elements is less than or equal to 1. The sign '*' represents the corresponding terms in two vectors multiplied and the result is still a vector. Let the s-th element in vector $\boldsymbol{e}$ be variable x, $x \in [-1,1]$, and the other elements are all fixed at 0. Then let

$$\begin{aligned} \boldsymbol{X}^s = \{0,\cdots,x,\cdots,0\}^{\mathrm{T}}, \quad s = 1,2,\cdots,m \\ 1,\cdots,s,\cdots,m \end{aligned} \tag{26}$$

and

$$\boldsymbol{h}^s = \boldsymbol{h}^c + \Delta\boldsymbol{h} * \boldsymbol{X}^s, \tag{27}$$

where the superscript 's' means the s-th interval variable is under analysis.

Our objective is to seek the bounds of the response statistics. In the same manner as in sect. 3, we first fix the frequency ω at the concerned frequency point $\omega=\omega_c$. Thus, the problem with two classes of variables is transformed into a problem containing only interval variables. For the symbol convenience, we write the component of response statistics matrix $S_{x_i x_j}(\boldsymbol{h}, \omega_c)$ as the simple formula $S(\boldsymbol{h})$ or S.

We introduce the first class Chebyshev polynomials:

$$T_n(x) = \cos(n \arccos x), \quad -1 \leqslant x \leqslant 1 \tag{28}$$

in which n is a nonnegative integer. $\{T_n(x)\}$ is a series of orthogonal polynomials with weight function $\dfrac{1}{\sqrt{1-x^2}}$, and satisfies recurrence relation as follows:

$$\begin{aligned} &T_0(x) = 1, \\ &T_1(x) = x, \\ &T_{n+1}(x) = 2xT_n(x) - T_{n-1}(x), \quad (n = 1,2,\cdots). \end{aligned} \tag{29}$$

Supposing $H_r = \mathrm{Span}\{T_0, T_1, \cdots, T_r\}$ is a subspace included in $C[-1,1]$, then we can choose the approximate polynomial $P_r(x) \in H_r$, such that

$$P_r(x) = \frac{a_0}{2} + \sum_{j=1}^{r} a_j T_j(x), \tag{30}$$

where

$$a_0 = \frac{2}{\pi}\int_{-1}^{1} \frac{S(h^s)}{\sqrt{1-x^2}}\mathrm{d}x, \tag{31}$$

$$a_j = \frac{2}{\pi}\int_{-1}^{1} \frac{S(h^s)T_j(x)}{\sqrt{1-x^2}}\mathrm{d}x, \quad j = 1,2,\cdots,r. \tag{32}$$

According to the Gauss-Chebyshev quadrature formula:

$$a_0 = \frac{2}{\pi}\int_{-1}^{1} \frac{S(h^s)}{\sqrt{1-x^2}}\mathrm{d}x \approx \sum_{k=1}^{q} A_k S(h_k^s), \tag{33}$$

$$a_j = \frac{2}{\pi}\int_{-1}^{1} \frac{S(h^s)T_j(x)}{\sqrt{1-x^2}}\mathrm{d}x \approx \sum_{k=1}^{q} A_k S(h_k^s) T_j(x_k), \tag{34}$$

where quadrature nodes $x_k, k = 1,2,\cdots,q$ are zero roots of $T_q(x)$, represented as:

$$x_k = \cos\frac{2(q-k)+1}{2q}\pi, \quad k = 1,2,\cdots,q, \tag{35}$$

and A_k are quadrature coefficients, represented as:

$$A_k = \int_{-1}^{1} \frac{T_q(x)}{\sqrt{1-x^2}(x-x_k)T_q'(x_k)}\mathrm{d}x = \frac{\pi}{q}, \quad k = 1,2,\cdots,q \tag{36}$$

and

$$h_k^s = h^s\big|_{x=x_k}. \tag{37}$$

Substituting eq. (36) into eqs. (33) and (34), we can obtain

$$a_0 = \frac{2}{q}\sum_{k=1}^{q} S(h_k^s), \tag{38}$$

$$a_j = \frac{2}{q}\sum_{k=1}^{q} S(h_k^s) T_j(x_k), \quad j = 1,2,\cdots,r. \tag{39}$$

Substituting eqs. (38) and (39) into eq. (30), we get

$$P_r(x) = \frac{1}{q}\sum_{k=1}^{q} S(h_k^s) + \frac{2}{q}\sum_{j=1}^{r}\sum_{k=1}^{q} S(h_k^s) T_j(x_k) T_j(x). \tag{40}$$

Let $S_k^s = S(h_k^s)$, eq. (40) can be rewritten as matrix form:

$$P_r(x) = \frac{2}{q}\left[S_1^s, S_2^s, \cdots S_q^s\right] \times \begin{bmatrix} 1/2 & T_1(x_1) & T_2(x_1) & \cdots & T_r(x_1) \\ 1/2 & T_1(x_2) & T_2(x_2) & \cdots & T_r(x_2) \\ 1/2 & \vdots & \vdots & \ddots & \vdots \\ 1/2 & T_1(x_q) & T_2(x_q) & \cdots & T_r(x_q) \end{bmatrix} \begin{bmatrix} T_0(x) \\ T_1(x) \\ T_2(x) \\ \vdots \\ T_r(x) \end{bmatrix}. \tag{41}$$

Let

$$\boldsymbol{S}^s = \left[S_1^s, S_2^s, \cdots S_q^s\right], \tag{42}$$

$$\boldsymbol{T} = \begin{bmatrix} 1/2 & T_1(x_1) & T_2(x_1) & \cdots & T_r(x_1) \\ 1/2 & T_1(x_2) & T_2(x_2) & \cdots & T_r(x_2) \\ 1/2 & \vdots & \vdots & \ddots & \vdots \\ 1/2 & T_1(x_q) & T_2(x_q) & \cdots & T_r(x_q) \end{bmatrix}, \tag{43}$$

$$\boldsymbol{T}(x) = \left[T_0(x) \quad T_1(x) \quad T_2(x) \quad \cdots \quad T_r(x)\right]^{\mathrm{T}}, \tag{44}$$

and

$$\boldsymbol{A}^s = \frac{2}{q}\boldsymbol{S}^s\boldsymbol{T}, \tag{45}$$

then $P_r(x)$ can be rewritten as:

$$P_r(x) = \boldsymbol{A}^s\boldsymbol{T}(x), \tag{46}$$

where $\boldsymbol{A}$ is a row vector and $\boldsymbol{T}(x)$ is a column vector.

In order to find the maximum and minimum value points of the objective function when the *s*-th interval available varies, it is necessary to obtain the extreme value point of the approximate function. We can accomplish this through seeking the roots of derived function and combining the function values at the interval bounds. The maximum and minimum value points of the *s*-th interval available are regarded as $r_{\max}^s$ and $r_{\min}^s$. Then traversing *s* from 1 to *m*, we can obtain the maximum and minimum points of the objective function with respect to each interval available. Let

$$\boldsymbol{h}_{\max} = \left[r_{\max}^1, r_{\max}^2, \cdots, r_{\max}^m\right]^{\mathrm{T}}, \tag{47}$$

$$\boldsymbol{h}_{\min} = \left[r_{\min}^1, r_{\min}^2, \cdots, r_{\min}^m\right]^{\mathrm{T}}. \tag{48}$$

Then bounds of the objective function can be derived from these points as:

$$\overline{S}(\boldsymbol{h}) = S(\boldsymbol{h}_{\max}), \tag{49}$$

$$\underline{S}(\boldsymbol{h}) = S(\boldsymbol{h}_{\min}). \tag{50}$$

4.2 Computational effort

First, we research how to choose the number of truncation terms *r* and the number of Gauss integral points *q*. Supposing $f(x)$ is a *r*-order polynomial, according to the Gauss-Chebyshev quadrature formula, we obtain

$$\int_{-1}^{1} \frac{f(x)}{\sqrt{1-x^2}}\mathrm{d}x = \frac{\pi}{q}\sum_{k=1}^{q} f\left(\cos\frac{2(r-k)+1}{2q}\pi\right), \tag{51}$$

and the truncation error is

$$R = \frac{f^{(2q)}(\xi)}{a_q^2(2q)!}\int_{-1}^{1}\frac{T_q^2(x)}{\sqrt{1-x^2}}\mathrm{d}x = \frac{2\pi}{2^{2q}(2q)!}f^{(2q)}(\xi), \quad \xi \in (-1,1). \tag{52}$$

When *r* is an odd number, the (*r*+1)-order derivative of *f*(*x*) is zero, that's to say, the truncation error characterized by eq. (52) will be zero when $q \geqslant (r+1)/2$. On the other hand, when *r* is an even number, the truncation error is not zero until $q \geqslant (r+2)/2$. Theoretically, the larger *r* is, the more accurate the obtained result is. It is suggested that odd numbers in 3–11 are chosen for *r* value in engineering. Thus, it can be seen that the truncation error will be zero as long as *q* is no less than 6. In general, Gauss quadrature formula with ten integral points is widely used in scientific calculations and can obtain high-accuracy integral results. Therefore, in the study we choose *q*=10.

The main computational effort is $\boldsymbol{S}^s$, defined by eq. (42) via the collocation interval analysis method. It is necessary to solve deterministic parameters structural system by *q* times in order to find the maximum and minimum value points of the objective function in the *s*-th interval variable. If the number of uncertain parameters is *m*, *m*×*q* times analysis is necessary.

It is remarkable that calculating matrix $\boldsymbol{T}$ defined by eq. (43) occupies little CPU time and can be neglected compared with the computational effort for calculating $\boldsymbol{S}^s$. The order of truncation polynomial *r* only contributes to computational accuracy, but requires barely any computational effort.

5 Determination of variance function interval

Once the PSD functions of response functions are obtained,

one can get the variance functions from integration

$$\boldsymbol{\sigma}_{xx}^2(t)=\frac{1}{2\pi}\int_{-\infty}^{\infty}\boldsymbol{S}_{xx}(\omega)\mathrm{d}\omega=\frac{1}{\pi}\int_{0}^{\infty}\boldsymbol{S}_{xx}(\omega)\mathrm{d}\omega$$
$$=\frac{1}{4\pi}\int_{0}^{\infty}\boldsymbol{G}_{xx}(\omega)\mathrm{d}\omega, \tag{53}$$

where $\boldsymbol{G}_{xx}(\omega)=2\boldsymbol{S}_{xx}(\omega)$ is single side PSD functions usually used in engineering.

Sects. 3 and 4 present two different methods to determine the bounds of PSD of response function at concerned frequency $\omega=\omega_c$, respectively. In this section, the interval of PSD of response function at concerned frequency $\omega=\omega_c$ is regarded as known:

$$S_{x_ix_i}^I(\boldsymbol{h},\omega_c)=\left[\underline{S}_{x_ix_i}(\boldsymbol{h},\omega_c),\overline{S}_{x_ix_i}(\boldsymbol{h},\omega_c)\right]. \tag{54}$$

As mentioned in eq. (53), variance function can be integrated from PSD function.

If the truncated frequency point for numerical integration operation is $\omega=\pm\omega_t$, we use the Gauss quadrature formula to integrate auto PSD to obtain a variance function of response. Completing the transformation

$$\omega=\frac{-\omega_t+\omega_t}{2}+\frac{\omega_t-(-\omega_t)}{2}z=\omega_t z, \tag{55}$$

thus

$$\overline{\sigma}_{x_i}^2=\frac{\omega_t}{2\pi}\int_{-1}^{1}\overline{S}_{x_ix_i}(\boldsymbol{h},\omega_t z)\mathrm{d}z, \tag{56}$$

$$\underline{\sigma}_{x_i}^2=\frac{\omega_t}{2\pi}\int_{-1}^{1}\underline{S}_{x_ix_i}(\boldsymbol{h},\omega_t z)\mathrm{d}z. \tag{57}$$

Collocate Gauss integral points in interval [−1, 1], and use Gauss quadrature formula to obtain the numerical solution of the bounds of variance function.

6 Numerical application

Firstly, we use a simple example to illuminate that the collocation interval analysis method presented in this paper can predict more accurate bounds of response than that obtained from the interval analysis method based on the first order Taylor expansion. Then, two examples from building under seismic ground motion excitation and aerofoil under continuous atmosphere turbulence excitation are presented to show the effectiveness of the proposed method.

6.1 A simple beam excited by moment at the center

In this example, the load is regarded as deterministic or containing interval parameters to show the accuracy of the collocation interval analysis method. A simple beam, depicted in Figure 2, is excited by a moment m at the center position. The Young's modulus of material $\boldsymbol{E}$ and the load value m are assumed to be discussed parameters. The values of the other parameters can be found in Table 1.

An analytical solution can be found to this problem. The deflection curve $v(x)$ and rotation angle $\theta(x)$ are

$$\begin{aligned} v(x)&=\frac{mx}{24EIL}(L^2-4x^2), \quad 0\leqslant x\leqslant\frac{L}{2},\\ \theta(x)&=v'(x), \qquad\qquad\qquad 0\leqslant x\leqslant\frac{L}{2}. \end{aligned} \tag{58}$$

The beam is divided into four straight beam elements and five nodes; we collocate nodes at the extreme value point and the center of the beam to reduce discretization errors. Three cases are discussed as follows:

(1) E is an interval variable, E^c=210000 MPa, ΔE=0.1E_0, m=100000 N mm;

(2) E is an interval variable, E^c=210000 MPa, ΔE=0.3E_0, m=100000 N mm;

(3) E is an interval variable, E^c=210000 MPa, ΔE=0.3E_0, m=100000sin(x^I) N mm, x^I=[1,3].

The results calculated by the three methods, namely, the Endpoints combination method (EPM), the interval analysis method based on the first order Taylor expansion (TIAM) and the collocation interval analysis method (CIAM), are shown in Tables 2–4 under different cases. The vertical displacement values of nodes 1, 3, and 5 and the angle of rotation of nodes 2 and 4 are all zero, so only non-zero displacement values are given in tables.

The displacement function is monotonic with respect to the uncertain parameters in case 1 and case 2. Tables 2 and 3 show that the bounds estimated by TIAM do not coincide well with the exact bounds. The results for one go beyond the actual bounds, and the other is not enough. Errors estimated by TIAM increase with the increase of interval radius of uncertain parameters. Although EPM can give exact bound values when the response is monotonic with respect to the uncertain parameters, it does not have the same effect

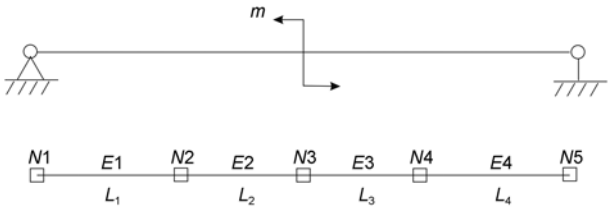

Figure 2 A simple beam excited by the moment at the center and its finite element model.

Table 1 Structure parameters of the beam

b (mm)	h (mm)	L (mm)
3	5	1000

Table 2 Comparison of the bounds by three methods with exact bound in case 1

Node	Nominal	Exact		Endpoints		TIAM		CIAM	
		upper	lower	upper	lower	upper	lower	upper	lower
1	–0.6349	–0.5772	–0.7055	–0.5772	–0.7055	–0.5714	–0.6984	–0.5772	–0.7055
2	–122.19	–111.08	–135.77	–111.08	–135.77	–109.97	–134.41	–111.08	–135.77
3	1.2698	1.4109	1.1544	1.4109	1.1544	1.3968	1.1429	1.4109	1.1544
4	122.19	135.77	111.08	135.77	111.08	134.41	109.97	135.77	111.08
5	–0.6349	–0.5772	–0.7055	–0.5772	–0.7055	–0.5714	–0.6984	–0.5772	–0.7055

Table 3 Comparison of the bounds by three methods with exact bound in case 2

Node	Nominal	Exact		Endpoints		TIAM		CIAM	
		upper	lower	upper	lower	upper	lower	upper	lower
1	–0.6349	–0.4884	–0.9070	–0.4884	–0.9070	–0.4444	–0.8254	–0.4884	–0.9070
2	–122.19	–93.99	–174.56	–93.99	–174.56	–85.53	–158.85	–93.99	–174.56
3	1.2698	1.8141	0.9768	1.8141	0.9768	1.6508	0.8889	1.8141	0.9768
4	122.19	174.56	93.99	174.56	93.99	158.85	85.53	174.56	93.99
5	–0.6349	–0.9070	–0.4884	–0.9070	–0.4884	–0.4444	–0.8254	–0.9070	–0.4884

Table 4 Comparison of the bounds by three methods with exact bound in case 3

Node	Nominal	Exact		Endpoints		TIAM		CIAM	
		upper	lower	upper	lower	upper	lower	upper	lower
1	–0.5773	–0.0689	–0.9070	–0.0689	–0.7632	–0.1399	–1.0148	–0.0689	–0.9070
2	–111.11	–13.26	–174.59	–13.26	–146.89	–26.93	–195.29	–13.26	–174.59
3	1.1547	1.8141	0.1378	1.5265	0.1378	2.0295	0.2798	1.8141	0.1378
4	111.11	174.56	13.26	146.89	13.26	195.29	26.93	174.56	13.26
5	–0.5773	–0.0689	–0.9070	–0.0689	–0.7632	–0.1399	–1.0148	–0.0689	–0.9070

when the response function loses the monotonicity. This can be seen from case 3 shown in Table 4. CIAM can give almost or same result with an exact solution in all cases with r=9.

6.2 A building excited by seismic ground motion

In engineering, seismic computations of building design have long been an issue of great concern. Owing to the randomness in the nature of seismic motions, responses of buildings can be analyzed using the random-vibration approach. In this section, a n - DOF building system in Figure 3 subjected to a stationary random seismic excitation is considered and the parameters are: m_i=m, k_i=k except for m_n=0.5m, k_1=2k. The damping coefficients c_i are consistent with Reyleigh damping, and the Reyleigh damping coefficients are α=0.1, β=0.2. The PSD of the stationary random process $x(t)$ has the Kanai-Tajimi form:

$$S_{xx}(\omega)=\frac{1+4(\zeta_g\omega/\omega_g)^2}{(1-\omega^2/\omega_g^2)^2+4(\zeta_g\omega/\omega_g)^2}S_0, \qquad (59)$$

where $\omega_g=19.07$ s^{-1}, $\zeta_g=0.544$ and $S_0=0.1574$ m^2 s^{-3}, as Figure 4 shows.

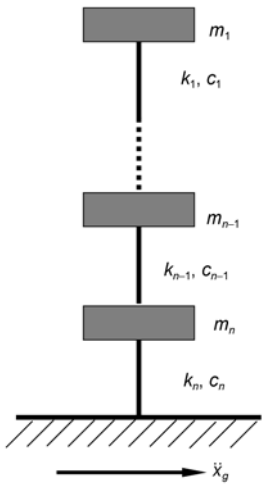

Figure 3 A building excited by seismic ground motion.

In the example, m and k have been assumed to be interval parameters with interval number $m^I=[m^c-\chi m^c, m^c+\chi m^c]$ and $k^I=[k^c-\eta k^c, k^c+\mu k^c]$ where $m^c=10^4$ kg and $k^c=1.4\times10^7$ kg/s^2 and χ, η are variable coefficients defining the deviation amplitude.

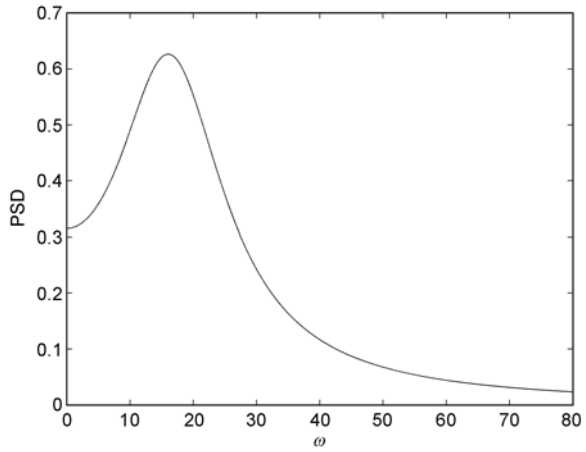

Figure 4 PSD of Kanai-Tajimi form (single side).

Figure 5(a) shows the bounds of PSD of m_1 obtained from different methods in the case of χ=0.1, η=0. Figure 5(b) shows that in the case of χ=0, η=0.1. Figures 5(c) and (d) show the comparison of the bounds of PSD of m_1 in the case of χ=0.1, η=0.1 and χ=0.2, η=0.2, respectively. It can be seen from Figure 5 that the bounds obtained from the two methods don't have an inclusion relation. In the main energy region of PSD, the bounds obtained from CIAM are higher than those obtained from TIAM. However, a reverse conclusion can be drawn in the low energy region. The bounds obtained from the two methods have fewer differences, shown in Figures 5(a) and (b), when the number of uncertainty variables and the located intervals are all small. However, as the number of uncertainty variables increases, the differences between the two methods grow, too, as Figure 5(c) shows. Furthermore, the bounds obtained from TIAM may make no sense in physics when the intervals are not small, which is seen from Figure 5(d). The lower bound obtained from TIAM is less than zero at some frequency points.

For the validation of CIAM, an optimization method is used to calculate the upper bound and lower bound, which can be treated as an exact solution. The comparison of CIAM and the OPT method are depicted in Figure 6. And Figure 6(a) shows that in the case of χ=0.1, η=0.1; Figure 6(b) shows that in the case of χ=0.2, η=0.2. It can be seen from Figure 6 that the bounds obtained from CIAM are consistent with the exact solution. Figure 7 shows the variances obtained from different methods in the case of χ=0, η: 0→0.2 and χ: 0→0.2, η=0. It can be seen that the variances obtained from TIAM are symmetrical at different sides of the nominal value. However, the nonlinear nature

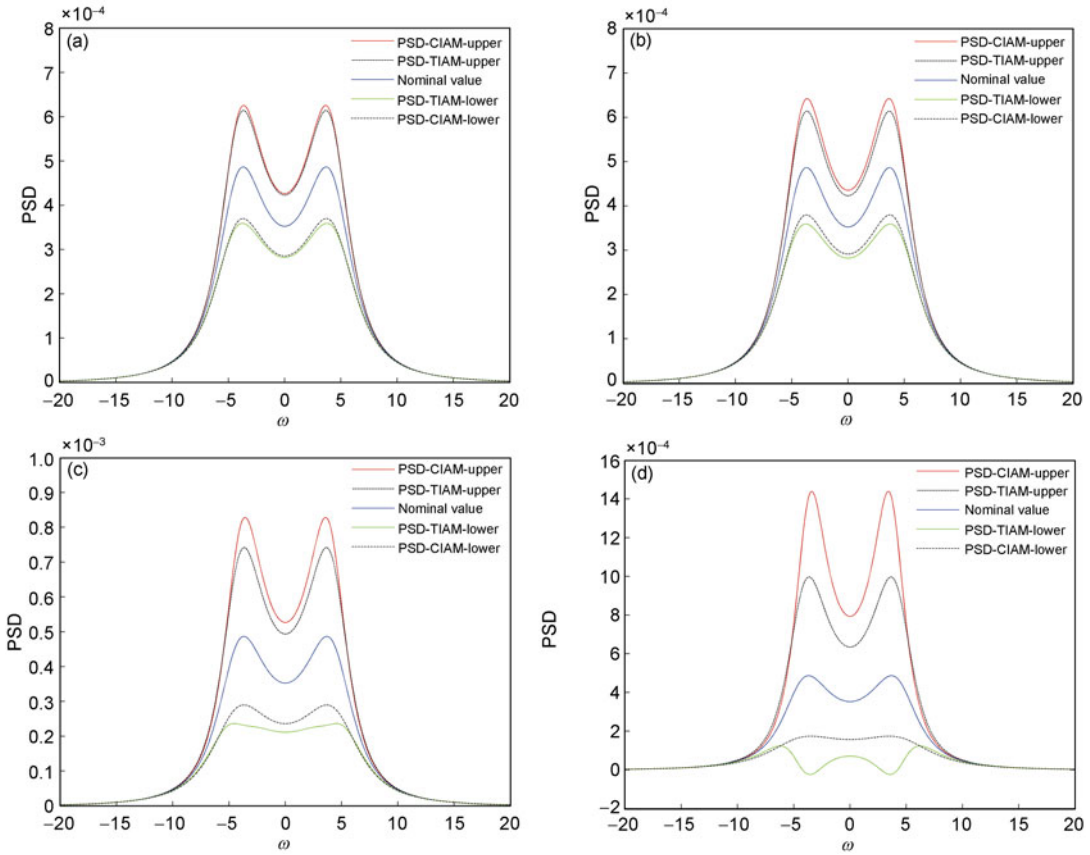

Figure 5 Comparison of the bounds obtained from TIAM and CIAM in different cases. (a) χ=0.1, η=0; (b) χ=0, η=0.1; (c) χ=0.1, η=0.1; (d) χ=0.2, η=0.2.

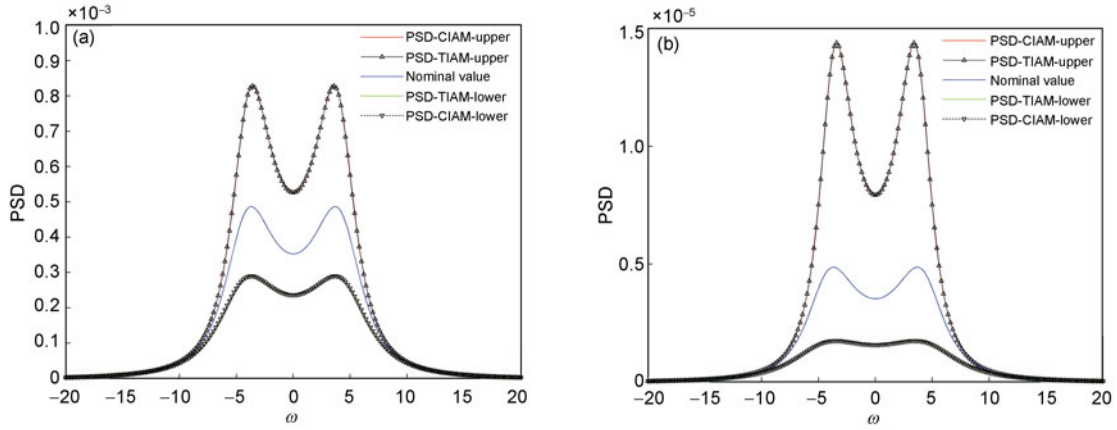

Figure 6 Comparison of the bounds obtained from CIAM and the optimization method in different cases. (a) χ=0.1, η=0.1; (b) χ=0.2, η=0.2.

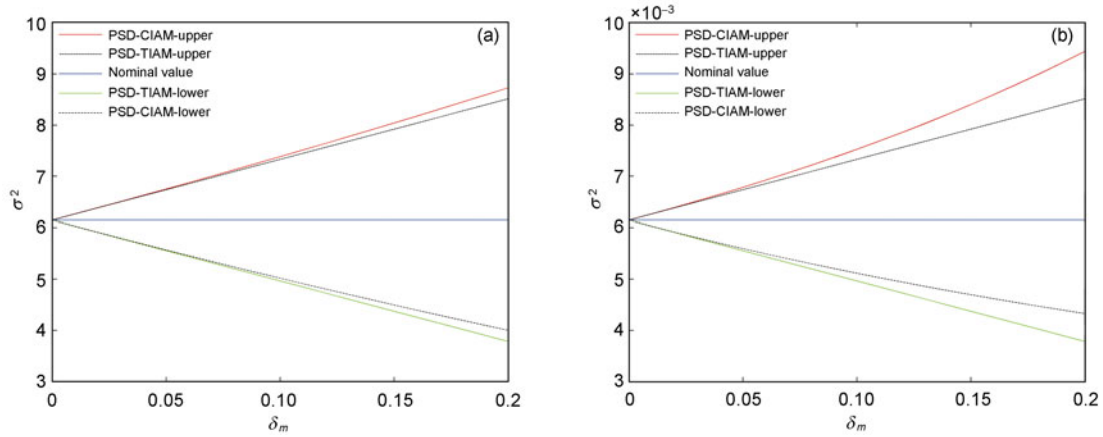

Figure 7 Variance comparison obtained from TIAM and CIAM methods in different cases. (a) χ=0, η: 0→0.2; (b) χ: 0→0.2, η=0.

can be observed using CIAM.

6.3 Aerofoil under continuous atmosphere turbulence excitation

Gust excitation, which can be modeled as discrete gust and continuous gust, plays an important role in aircraft design. Continuous gust is considered a stationary random process in mathematics. In this section, we consider a simplified aerofoil model, the FEM model (Figure 8), which contains 656 nodes and 640 shell elements. The vertical gust velocity in continuous atmosphere turbulence is described by Dryden PSD (single side) depicted in Figure 9. For the sake of simplicity, only the translational motion caused by transient aerodynamic force and gust is considered to introduce the aeroelasticity effect. The Theodorsen theory is adopted for calculating the transient aerodynamic force. The Young's modulus of material E and shell thickness t is treated as interval variables with E^c=0.7×10^{11} Pa and t^c=3 mm. The other parameter values are listed in Table 5, where ρ_a and ρ_m are the density of air and material of aerofoil, respectively. L_s is the gust scale, L is the half length of wingspan,

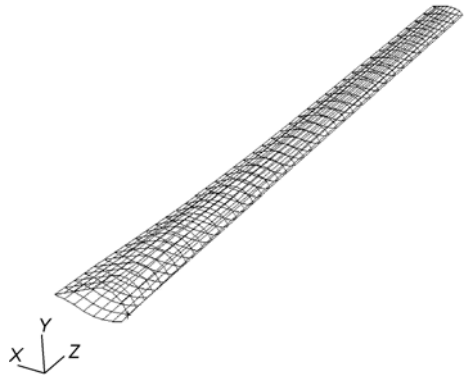

Figure 8 Straight wing finite element model.

V is the flight speed, and α, β are the Reyleigh damping coefficients.

Figure 10(a) shows the bounds of PSD of wing tip obtained from TIAM and CIAM in the case of χ=0.1, η=0. Figure 10(b) shows that in the case of χ=0, η=0.1. Figures 10(c) and (d) show the bounds of PSD of wing tip obtained from different methods in the case of χ=0.1, η=0.1

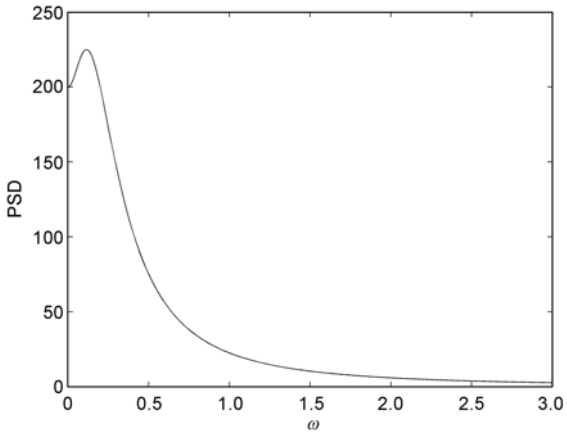

Figure 9 Dryden PSD (single side).

and χ=0.2, η=0.2, respectively. Here the meaning of χ and η is the same as in sect. 6.2. From Figure 10, we conclude that the bounds obtained from TIAM are the located symmetric position at the sides of nominal value while the results obtained from CIAM are not. In the same manner as in sect. 6.2, we use the optimization method to get the exact bounds to examine the validation of CIAM, as shown in Figure 11.

7 Conclusion

We study the response statistics of engineering structures with interval parameters under stationary random excitation using the interval analysis method. The analysis of "point approximation" interval finite element method based on the first order Taylor expansion shows that TIAM is only suited for the case for the narrow interval hypothesis. However, CIAM—which adopts a non-gradient algorithm based on several collocation points—can break through the restrictions on TIAM use and improve the precision of results via the interval analysis method. The main computational effort lies in calculating the values of objective function at Gaussian integration points. Compared with the results obtained

Table 5 Parameters of the aeroelastic system

ρ_a (kg/m^3)	ρ_m (kg/m^3)	V (m/s)	L_s (m)	L (m)	α	β
1.225	7800	200	1000	23.2	0.002	0.002

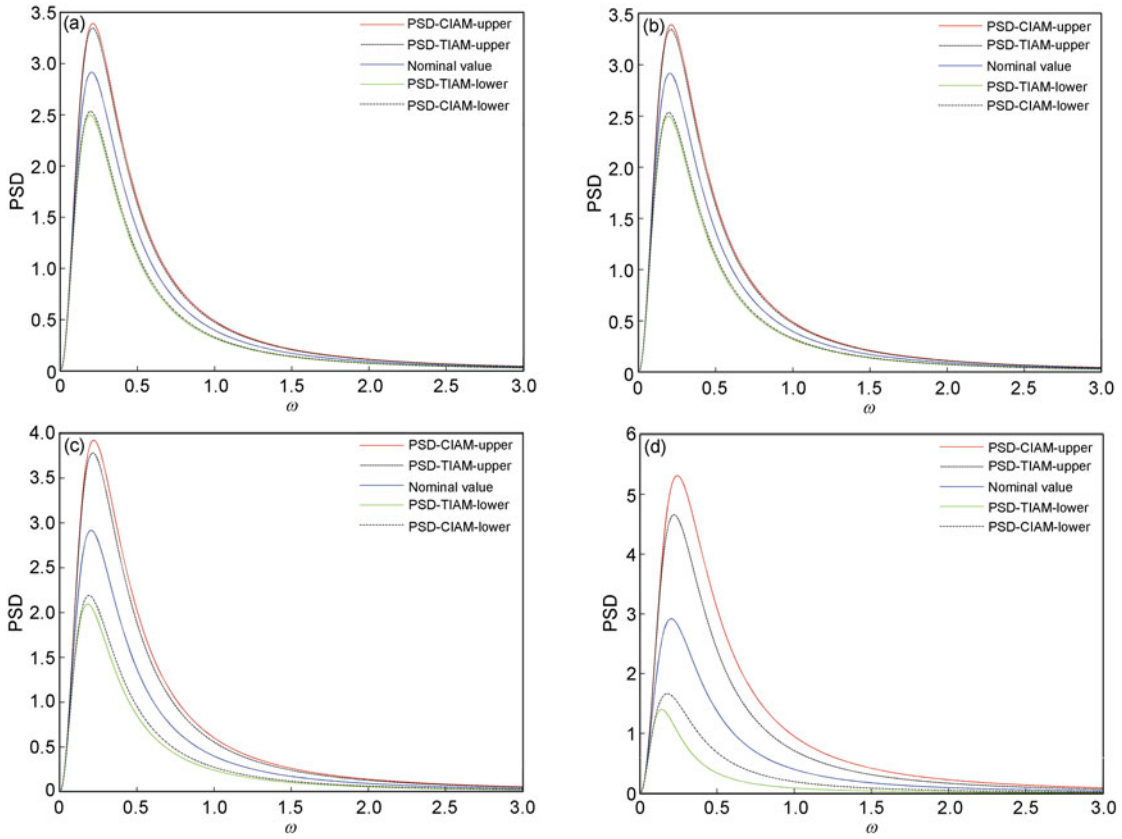

Figure 10 Comparison of the bounds obtained from TIAM and CIAM in different cases. (a) χ=0.1, η=0; (b) χ=0, η=0.1; (c) χ=0.1, η=0.1; (d) χ=0.2, η=0.2.

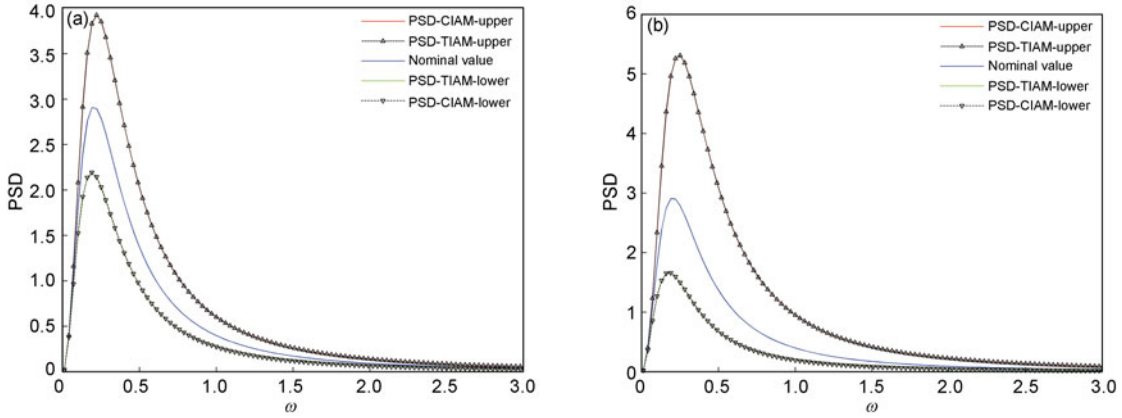

Figure 11 Comparison of the bounds obtained from CIAM and the optimization method in different cases. (a) χ=0.1, η=0.1; (b) χ=0.2, η=0.2.

from the optimization method, the proposed method yields high precision approximation to the exact solution, but takes little computational effort.

This work was supported by the National Natural Science Foundation of China (Grant Nos. 10872017, 90816024 and 10876100) and 111 Project (Grant No. B07009).

1 Ibrahim R A. Structural dynamics with parameter uncertainties. Appl Mech Rev, 1987, 40(3): 309–328
2 Li J, Liao S T. Response analysis of stochastic parameter structures under non-stationary random excitation. Comput Mech, 2001, 27(1): 61–68
3 Papadopoulos C E, Yeung H. Uncertainty estimation and Monte Carlo simulation method. Flow Meas Instrum, 2001, 12(4): 291–298
4 Thunnissen D P, Au S K, Swenka E R. Uncertainty quantification in conceptual design via an advanced Monte Carlo method. J Aerospace Comput, 2007, 4(7): 902–917
5 Sepka S A, Wright M. A Monte Carlo approach to FIAT uncertainties improvements and applications For MSL. AIAA Paper, 2009, AIAA-2009-4234
6 Akram F, Prior M A, Mavris D N. A comparison between Monte Carlo and evidence theory approaches for technology portfolio planning. AIAA Paper, 2011, AIAA-2011-1412
7 Ishida R. Stochastic finite element analysis of beam with statistical uncertainties. AIAA J, 2001, 39(11): 2192–2197
8 Chung D B, Gutierrez M A, Remmers J J C, et al. Stochastic finite element modelling of fibre-metal laminates. AIAA Paper, 2004, AIAA-2004-1992
9 Onkar A K, Upadhyay C S, Yadav D. Stochastic finite element failure analysis of laminated plates under uniaxial compressive loading. AIAA Paper, 2006, AIAA-2006-2003
10 Adhikari S, Kundu A. A reduced spectral projection method for Stochastic finite element analysis. AIAA Paper, 2011, AIAA-2011-1846
11 Pettit C L. Sampling-based sensitivity analysis through proper orthogonal decomposition and cluster-weighted. AIAA Paper, 2008, AIAA-2008-1988
12 Nguyen N. Least-squares adaptive control using chebyshev orthogonal polynomials. AIAA Paper, 2011, AIAA-2011-1402
13 Moens D, Vandepitte D. A survey of non-probabilistic uncertainty treatment in finite element analysis. Comput Methods Appl Mech Eng, 2005, 194(12-16): 1527–1555
14 William S M. Anti-Optimization of uncertain structures using interval analysis. Comput Struct, 2011, 79(4): 421–430
15 Qiu Z P, Wang X J. Parameter perturbation method for dynamic response of structures with uncertain-but-bounded parameters based on interval analysis. Int J Solids Struct, 2005, 42(18-19): 4958–4970
16 Chen S H, Lian H D, Yang X W. Interval static displacement analysis for structures with interval parameters. Int J Numer Meth Eng, 2002, 53(2): 393–407
17 Qiu Z P. Comparison of static response of structures using convex models and interval analysis method. Int J Numer Eng, 2003, 56(1): 1735–1753
18 Moore R E, Kearfott R B, Cloud M J. Introduction to Interval Analysis. Philadelphia, PA: Society for Industrial and Applied Mathematics, 2009
19 Qiu Z P, Wang X J. Comparison of dynamic response of structures with uncertain-but-bounded parameters using nonprobabilistic interval analysis method and probabilistic approach. Int J Solids Struct, 2003, 40(20): 5423–5439
20 Wang X J. Qiu Z P. Interval finite element analysis of wing flutter. Chin J Aeronaut, 2008, 21(2): 134–140
21 Xia Y Y, Qiu Z P, Friswell M. The time response of structures with bounded parameters and interval initial conditions. J Sound Vib, 2010, 329(3): 353–365
22 Qiu Z P. Wang X J. Vertex solution theorem for the upper and lower bounds on the dynamic response of structures with uncertain-but-bounded parameters. Acta Mech Sin, 2009, 25(3): 367–379
23 Chen S H, Zhang X M. Dynamic response of closed-loop system with uncertain parameters using interval finite element method. Int J Numer Meth Eng, 2007, 70: 543–562
24 Lin J H, Zhang Y H. Seismic Random Vibration of Long-Span Structures. Boca Raton, FL: CRC Press, 2005
25 Lin J H, Zhao Y, Zhao Y H. Accurate and highly efficient algorithms for structural stationary/non-stationary random responses. Comput Methods Appl Mech Eng, 2001, 191(1-2): 103–111
26 Yi P, Lin J H, Zhao Y. Variation analysis of non-stationary random response of linear random structures (in Chinese). Acta Mech Solida Sin, 2002, 23(1): 93–97
27 Zhao Y, Lin J H, Guo X L. Seismic random vibration analysis of bridges with hysteretic nonlinearity (in Chinese). Chin J Comput Mech, 2005, 22(2): 145–148